

Synthesis and Reactivity of Silicon- and Germanium-Bridged *ansa*-Cycloheptatrienyl–Cyclopentadienyl Titanium Complexes

Matthias Tamm,* Andreas Kunst, Thomas Bannenberg, Sören Randoll, and Peter G. Jones

Institut für Anorganische und Analytische Chemie, Technische Universität Carolo-Wilhelmina, Hagenring 30, D-38106 Braunschweig, Germany

Received October 10, 2006

A new type of *ansa*-cycloheptatrienyl–cyclopentadienyl complex with germanium as a bridging atom has been synthesized. Using the established route for the formation of $[(\eta\text{-C}_5\text{H}_4)\text{Me}_2\text{Si}(\eta\text{-C}_7\text{H}_6)\text{Ti}]$, [1]-silatroticenophane **1**, the analogous germylene-bridged derivative $[(\eta\text{-C}_5\text{H}_4)\text{Me}_2\text{Ge}(\eta\text{-C}_7\text{H}_6)\text{Ti}]$ (**2**) has been isolated from the reaction of $[(\eta\text{-C}_7\text{H}_7)\text{Ti}(\eta\text{-C}_5\text{H}_5)]$ (troticene) with *n*-butyllithium/*N,N,N',N'*-tetramethylethylenediamine (tmeda) in hexane and subsequent treatment of the intermediate dilithio complex with dimethyl(dichloro)germane. [1]Germatroticenophane **2** has been isolated in yields up to 15–20% and was characterized by means of ^1H , ^{13}C NMR spectroscopy, elemental analysis, and mass spectrometry. In addition, an X-ray diffraction study on a single crystal of **2** has been performed, and the structural characteristics are discussed in comparison to related *ansa*-compounds. The differential scanning calorimetry trace of **2** shows a strong exotherm at about 130 °C, which is the result of a thermally induced ring-opening polymerization reaction, and a strain energy of about 45 kJ mol $^{-1}$ has been determined. The reaction of **2** with equivalent amounts of tris(triethylphosphine)platinum(0) involves a regioselective insertion of a $[\text{Pt}(\text{PEt}_3)_2]$ moiety into the germanium–carbon bond at the C $_7$ H $_6$ site, yielding the [2]platinasilagermatroticenophane $[(\eta\text{-C}_5\text{H}_4)\text{Me}_2\text{GePt}(\text{PEt}_3)_2(\eta\text{-C}_7\text{H}_6)\text{Ti}]$ (**10**), which was characterized by ^1H , ^{13}C , ^{31}P , and ^{195}Pt NMR spectroscopy. In addition, the reactivity of **1** toward protic acids such as HCl and HBF $_4$ has been investigated, yielding complexes of the type $[(\eta\text{-C}_7\text{H}_7)\text{Ti}(\eta\text{-C}_5\text{H}_4\text{SiMe}_2\text{X})]$ (X = Cl, F) by exclusive cleavage of the Si–C $_7$ H $_6$ silicon–carbon bond and protonation of the cycloheptatrienyl *ipso*-carbon atom.

Introduction

It was the serendipitous discovery of ferrocene, $[(\eta\text{-C}_5\text{H}_5)_2\text{Fe}]$, in 1951¹ and one year later the monumental elucidation of its sandwich-type structure by E. O. Fischer² and G. Wilkinson³ that triggered the remarkable development of cyclopentadienyl transition metal chemistry, which is still ongoing today. It is estimated that 80% of all organometallic complexes bear the cyclopentadienyl ligand (Cp) or its substituted derivatives.⁴ The importance of the Cp system can be attributed inter alia to the virtually unlimited possibilities of altering the steric and/or electronic properties of the resulting complexes by replacement of the hydrogen atoms in the parent C $_5$ H $_5$ system by alkyl or aryl substituents. As a result, the steric bulk, stability, and solubility of the Cp complexes can be influenced and hence directly adapted to the desired applications. Indeed, cyclopentadienyl metal complexes have found widespread use in many different research areas such as homogeneous catalysis,⁵

medicinal chemistry,⁶ and materials science.⁷ In particular, bridged bis(cyclopentadienyl) systems (*ansa*-metallocenes) with group 4 metal centers are used as reagents in organic synthesis and as components for the generation of very active and selective Ziegler–Natta catalysts for olefin polymerization.⁸ Moreover, highly strained *ansa*-metallocenes such as $[\text{Me}_2\text{Si}(\eta^5\text{-C}_5\text{H}_4)_2\text{Fe}]$ are excellent precursors for the generation of metallopolymers that have been shown to exhibit intriguing electrochemical, optical, thermal, and magnetic properties.⁹ In contrast, the organometallic chemistry of the cycloheptatrienyl ligand (Cht) has been little studied in comparison with that of the Cp system, although Cht complexes, $[(\eta\text{-C}_7\text{H}_7)\text{ML}_n]$, have been known for more than four decades.¹⁰

Only recently have we successfully introduced the well-known concept of ligand functionalization to Cht transition metal chemistry with the synthesis of linked cycloheptatrienylphos-

* Corresponding author. Tel: +49-531-3915309. Fax: +49-531-3915387. E-mail: m.tamm@tu-bs.de.

(1) (a) Keely, T. J.; Pauson, P. L. *Nature* **1951**, *168*, 1039. (b) Miller, S. A.; Tebboth, J. A.; Tremaine, J. F. *J. Chem. Soc.* **1952**, 632.

(2) Fischer, E. O.; Pfab, W. *Z. Naturforsch.* **1952**, *7b*, 377.

(3) Wilkinson, G.; Rosenblum, M.; Whiting, M. C.; Woodward, R. B. *J. Am. Chem. Soc.* **1952**, *74*, 2125.

(4) Janiak, C.; Schumann, H. *Adv. Organomet. Chem.* **1991**, *33*, 331.

(5) (a) *Applied Homogeneous Catalysis with Organometallic Compounds*; Cornils, B., Herrmann, W. A., Eds.; Wiley-VCH: Weinheim, 1996. (b) Herrmann, W. A.; Cornils, B. *Angew. Chem.* **1997**, *109*, 1074; *Angew. Chem., Int. Ed. Engl.* **1997**, *36*, 1048. (c) Britovsek, G. J. P.; Gibson, V. C.; Wass, D. F. *Angew. Chem.* **1999**, *111*, 448; *Angew. Chem., Int. Ed.* **1999**, *38*, 428. (d) Gibson, V. C.; Spitzmesser, S. K. *Chem. Rev.* **2003**, *103*, 283. (e) Gladysz, J. A., Ed. Special Volume “Frontiers in Metal-Catalyzed Polymerization”. *Chem. Rev.* **2000**, *100* (4).

(6) (a) Köpf-Maier, P.; Köpf, H. *Struct. Bond.* **1988**, *70*, 105. (b) Caruso, F.; Rossi, M. *Met. Ions Biol. Syst.* **2004**, *42*, 353. (c) Caruso, F.; Rossi, M. *Minirev. Med. Chem.* **2004**, *4*, 49.

(7) *Inorganic Materials*; Bruce, D. W., O'Hare, O., Eds.; Wiley: Chichester, 1992.

(8) (a) Wang, B. *Coord. Chem. Rev.* **2006**, *250*, 242. (b) Shapiro, P. *Coord. Chem. Rev.* **2002**, *231*, 67.

(9) (a) *Inorganic and Organometallic Polymers*; Chandrasekhar, V., Ed.; Springer-Verlag GmbH & Co. KG: Heidelberg, 2005. (b) Nguyen, P.; Gomez-Elipse, P.; Manners, I. *Chem. Rev.* **1999**, *99*, 1515. (c) *Synthetic Metal Containing Polymers*; Manner, I., Ed.; Wiley-VCH: Weinheim, 2004. (d) *Macromolecules Containing Metal and Metal-Like Elements*; Abd-el-Aziz, A. S., Carraher, C. E., Jr., Pittman, C. U., Jr., Sheats, J. E., Zeldin, M., Eds.; Wiley: New York, 2004; Vols. 1–3. (e) *Inorganic and Organometallic Polymers*; Archer, R. D., Ed.; Wiley: New York, 2001. (f) Manners, I. *Science* **2001**, *294*, 1664.

(10) Green, M. L. H.; Ng, D. K. P. *Chem. Rev.* **1995**, *95*, 439.

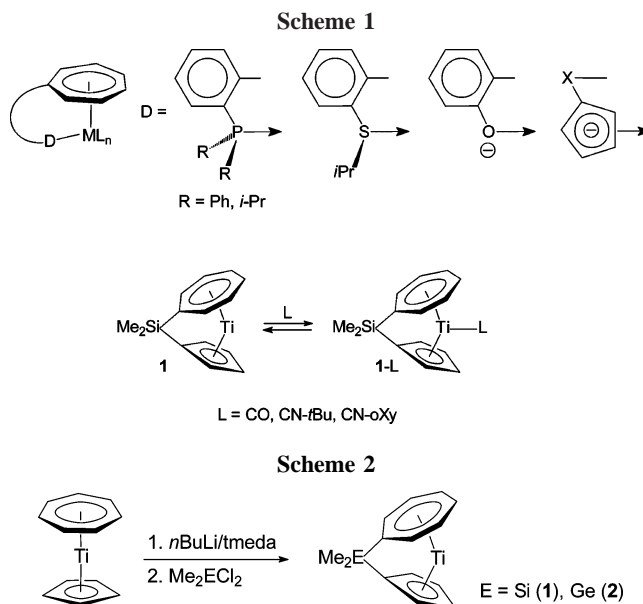
phane,¹¹ -thiolate,¹² and -phenolate ligands.¹³ While completing these studies, we became interested in the preparation of bridged Cht–Cp sandwich complexes, in which the ligand can be regarded as a Cp-donor-functionalized cycloheptatrienyl ligand, and have communicated the synthesis of the silicon-bridged *ansa*-Cht–Cp titanium complex the [1]silatrotrocenophane **1**. It was demonstrated that this highly strained molecule is susceptible to strain release by ring-opening polymerization (ROP) reactions.¹⁴ In addition, bridging of the carbocyclic ligands in **1** creates a gap at the metal center, which thereby becomes accessible to slender σ -donor/ π -acceptor ligands such as carbon monoxide and isocyanides.¹⁵ The experimental and theoretical investigation of these metal–ligand interactions revealed that the titanium center in **1** bears a closer resemblance to Lewis acidic Ti^{IV} rather than Ti⁰. Accordingly, the Cht ring functions more as a trinegative 10-electron ligand than as the more common tropylium cation,^{15–17} a description that has also been confirmed in the related Cp–Cht zirconium complex trozircene.^{18,19}

With this contribution, we wish to report the synthesis and characterization of the germanium-bridged congener of **1**, namely, the [1]germatrotrocenophane **2**. Additionally, the reactivity of the single-atom bridge in **1** and **2** toward ring-opening polymerization, transition metal insertion, and protonolysis reactions has been studied and is described herein.

Results and Discussion

Synthesis and Characterization of *ansa*-Cht–Cp Complexes. The *ansa*-Cht–Cp complex [1]germatrotrocenophane **2** can be obtained in a similar way to that described for the synthesis of **1**.¹⁵ Reaction of $[(\eta^7\text{-C}_7\text{H}_7)\text{Ti}(\eta^5\text{-C}_5\text{H}_5)]$ (troticene)²⁰ with *n*-butyllithium/*N,N,N',N'*-tetramethylethylenediamine (tmeda) followed by treatment of the intermediate dilithio complex²¹ with dimethyl(dichloro)germane leads to the formation of **2** in moderate yields of 15–20% after crystallization from hexane (Scheme 2).

The blue complex proved to be very sensitive toward air and moisture, but can be stored at room temperature in an anaerobic atmosphere for a long period of time without degradation. The ¹H NMR spectrum of **2** in benzene-*d*₆ exhibits a splitting pattern



of the C₇H₆ and the C₅H₄ resonances that suggests the formation of a C_s-symmetric complex. The former two singlet signals in trocicene at 5.42 (C₇H₇) and 4.90 ppm (C₅H₅) are now split into five resonances in a ratio of 2:2:2:2:2, and in contrast to **1**, all C₅H₄ and C₇H₆ resonances are well resolved (Figure 1). The signals of the β - and γ -C₇H₆ protons in **2** are low-field shifted to 5.96 and 5.88 ppm in comparison to the unbridged trocicene, whereas the resonance of the α -C₇H₆ protons next to the bridging unit can be detected at higher field (4.76 ppm). The CH₃ resonance signal is observed at 0.50 ppm, slightly upfield from the corresponding resonance in **1** (0.41 ppm). As expected, the ¹³C NMR spectrum of the [1]germatrotrocenophane **2** has seven signals for the ring carbon atoms between 100.7 and 58.8 ppm, whereby the two upfield signals at 81.6 (*i*-C₅H₄) and 58.8 ppm (*i*-C₇H₆) can be unambiguously assigned to the *ipso*-carbon atoms. In **1**, the latter resonances are observed at slightly lower field (83.6 and 61.6 ppm), and a similar trend has also been observed for the resonances of the *ipso*-carbon atoms in [1]dimethylsilaferrocenophane (33.5 ppm)²² and [1]dimethylgermaferrocenophane (31.0 ppm).²³ In general, such remarkably large upfield shifts are characteristic for tilted sandwich structures and reflect strong distortions about the *ipso*-carbon–heteroatom bonds.²⁴

To compare the solid-state structures of the silicon- and germanium-bridged trocicene derivatives **1** and **2**, single-crystals of **2** were isolated from a saturated toluene solution at –35 °C, and the molecular structure was established by X-ray diffraction analysis. Compound **2** is isotopic to **1**; it crystallizes in *Pnma* with a mirror plane bisecting the titanium atom, the ring carbon

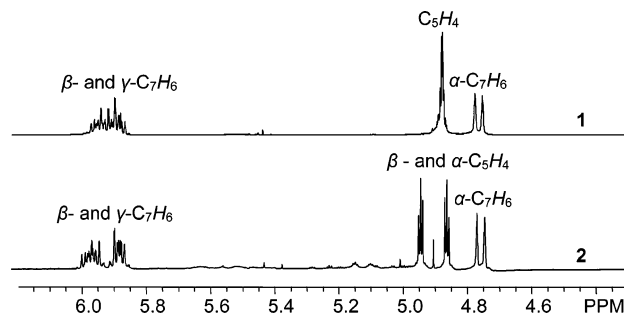


Figure 1. Excerpts from the ¹H NMR spectra of the [1]-silatrotrocenophane **1** (top) and the [1]germatrotrocenophane **2** (bottom) in benzene-*d*₆.

(11) (a) Tamm, M.; Baum, K.; Lügger, T.; Fröhlich, R.; Bergander, K. *Eur. J. Inorg. Chem.* **2002**, 918. (b) Tamm, M.; Dressel, B.; Urban, V.; Lügger, T. *Inorg. Chem. Commun.* **2002**, 5, 837. (c) Tamm, M.; Dressel, B.; Lügger, T.; Fröhlich, R.; Grimme, S. *Eur. J. Inorg. Chem.* **2003**, 1088. (d) Tamm, M.; Dressel, B.; Baum, K.; Lügger, T.; Pape, T. *J. Organomet. Chem.* **2003**, 677, 1. (e) Tamm, M.; Dressel, B.; Lügger, T. *J. Organomet. Chem.* **2003**, 684, 322.

(12) Tamm, M.; Dehn, S. Unpublished results.

(13) Tamm, M.; Bannenberg, T.; Dressel, B.; Fröhlich, R.; Holst, C. *Inorg. Chem.* **2002**, 41, 47.

(14) Tamm, M.; Kunst, A.; Herdtweck, E. *Chem. Commun.* **2005**, 1729.

(15) Tamm, M.; Kunst, A.; Bannenberg, T.; Herdtweck, E.; Elsevier, C. J.; Ernsting, J. M. *Angew. Chem.* **2004**, 116, 5646; *Angew. Chem., Int. Ed.* **2004**, 43, 5530.

(16) (a) Menconi, G.; Kaltsoyannis, N. *Organometallics* **2005**, 24, 1189.

(b) Kaltsoyannis, N. *J. Chem. Soc., Dalton Trans.* **1995**, 3727.

(17) Green, J. C.; Kaltsoyannis, N.; Sze, K. H.; MacDonald, M. *J. Am. Chem. Soc.* **1994**, 116, 1994.

(18) Tamm, M.; Kunst, A.; Bannenberg, T.; Herdtweck, E.; Schmid, R. *Organometallics* **2005**, 24, 3163.

(19) Baker, R.; Bannenberg, T.; Kunst, A.; Randoll, S.; Tamm, M. *Inorg. Chim. Acta* **2006**, 395, 4797.

(20) For the sandwich compound $[(\eta^7\text{-C}_7\text{H}_7)\text{Ti}(\eta^5\text{-C}_5\text{H}_5)]$, we introduced the trivial name *trocicene* (see refs 15 and 19), which stands for $[(\eta^7\text{-tropylium})\text{titanium}(\eta^5\text{-cyclopentadienyl})]$ and is in accord with the naming of $[(\eta^7\text{-C}_7\text{H}_7)\text{V}(\eta^5\text{-C}_5\text{H}_5)]$ as *trovacene*; see for instance: Elschenbroich, C.; Schiemann, O.; Burghaus, O.; Harms, K. *J. Am. Chem. Soc.* **1997**, 119, 7452.

(21) Ogasa, M.; Rausch, M. D.; Rogers, R. D. *J. Organomet. Chem.* **1991**, 403, 279.

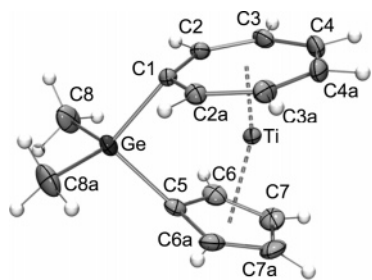


Figure 2. ORTEP-style plot of the molecular structure of **2**. Selected bond lengths [Å]: Ti–C1 2.176(2), Ti–C2 2.195(1), Ti–C3 2.227(2), Ti–C4 2.253(2), Ti–C5 2.311(2), Ti–C6 2.314(2), Ti–C7 2.349(2), C1–C2 1.433(2), C2–C3 1.428(2), C3–C4 1.418(2), C4–C4a 1.414(4), C5–C6 1.430(2), C6–C7 1.414(2), C7–C7a 1.411(4), Ge–C1 1.967(2), Ge–C5 1.969(2), Ge–C8 1.936(2), Ge–Ti 3.0903(4), Ti–C7 1.492, Ti–C5 1.990, symmetry operation to equivalent positions a: $x, 1/2-y, z$.

Table 1. Comparison of Selected Bond Lengths of Tropicene with **1** and **2**^a

	tropicene	1	2
Ti–C7 ^b	1.487	1.496	1.492
Ti–C7 ^c	2.212	2.219	2.218
average	2.202(1)–2.217(1)	2.170(3)–2.256(2)	2.176(2)–2.253(2)
range			
C7–C7 ^c	1.422	1.422	1.426
average	1.416(1)–1.427(1)	1.409(3)–1.436(3)	1.414(4)–1.433(2)
range			
Ti–Ct5 ^d	1.982	1.988	1.990
Ti–C5 ^e	2.333	2.326	2.327
average	2.321(1)–2.338(1)	2.294(3)–2.353(3)	2.311(2)–2.349(2)
range			
C5–C5 ^e	1.412	1.420	1.420
average	1.409(1)–1.414(1)	1.410(5)–1.435(3)	1.411(4)–1.430(2)
range			
Ti–E		3.008(1)	3.0903(4)

^a Bond lengths in Å. ^bC7 = centroid of the seven-membered ring. ^cC7 = carbon atom of the seven-membered ring. ^dCt5 = centroid of the five-membered ring. ^eC5 = carbon atom of the five-membered ring.

atoms C1 and C5, and the Ge atom of the bridging moiety. As expected, the Cht and the Cp rings are virtually planar and can be regarded as being essentially η^7 - and η^5 -coordinated, respectively. The carbon–metal bond distances to the seven-membered ring are significantly shorter than those to the five-membered ring [Ti–C7 = 2.176(2)–2.253(2) Å, Ti–C5 = 2.311(2)–2.349(2) Å], indicating a stronger interaction between the metal and the Cht ligand, as previously observed for the unbridged tropicene²⁵ and for the corresponding trozircene.¹⁸ The average metal–carbon distances to the seven-membered ring in **2** are only marginally longer than those in the unstrained tropicene (2.218 vs 2.212 Å), whereas the reverse trend is observed for the metal–carbon distances in the five-membered ring (2.327 vs 2.333 Å). Substitution of the silicon atom in **1** by germanium does not alter the structural parameters significantly, and all average Ti–C and C–C distances in **1** and **2** are identical within experimental error (Table 1). The Ti–Ge distance of 3.0903(4) Å lies well outside the range of the sum of the covalent radii (2.54 Å)²⁶ and is significantly longer than the bond lengths determined for germyl–titanium complexes,

(22) Finckh, W.; Tang, B.-Z.; Foucher, D. A.; Zamble, D. B.; Ziembinski, R.; Lough, A.; Manners, I. *Organometallics* **1993**, *12*, 823.

(23) Foucher, D. A.; Edwards, M.; Burrow, R. A.; Lough, A. J.; Manners, I. *Organometallics* **1994**, *13*, 4959.

(24) Osborne, A. G.; Whiteley, R. H.; Meads, R. E. *J. Organomet. Chem.* **1980**, *193*, 345.

(25) Lyssenko, K. A.; Antipin, M. Y.; Ketkov, S. Y. *Russ. Chem. Bull. Int. Ed.* **2001**, *50*, 130.

(26) Deb, B. M.; Singh, R.; Sukumar, N. *J. Mol. Struct.* **1992**, *259*, 121.

Table 2. Structural Comparison of Silylene- and Germylene-Bridged ansa-Complexes

compound	α /deg	β /deg, β' /deg	θ /deg	δ /deg
1	24.1	42.3, 29.2	95.6	160.5
2	22.9	41.4, 28.5	92.8	161.0
3	20.8	37.0	95.7	164.7
4	19.1	37.8, 35.9	91.7	n/a
5	16.6	38.2, 37.9	92.9	167.6
6	14.4	38.7	91.8	n/a
7	17.3	48.3, 32.6	98.2	167.0
8	15.6	47.7, 30.6	93.9	168.4

e.g., Ti–Ge = 2.710 Å in $[(\eta\text{-C}_5\text{H}_5)_2\text{Ti}(\text{GePh}_3)(\eta^2\text{-COCH}_3)]$ ²⁷ and Ti–Ge = 2.653 Å in $[(\text{Me}_2\text{N})_3\text{Ti}-\text{Ge}(\text{SiMe}_3)_3]$.²⁸ This suggests that no interaction between the metal center and the heteroatom is present in **2**, although crystallographic and ⁵⁷Fe Mössbauer spectroscopic studies on $[\text{Me}_2\text{Ge}(\eta\text{-C}_5\text{H}_4)_2\text{Fe}]$ revealed a weak dative interaction between iron and the germanium atom [$d(\text{Fe}-\text{Ge}) = 2.804(2)$ Å].²³

The degree of deviation from an unstrained sandwich structure with an ideal coplanar ring orientation can be characterized by the angles α , β , β' , θ , and δ , which are defined in Table 2. Since germanium has a larger covalent radius than silicon,²⁶ one would expect the [1]germatropicenophane **2** to be less distorted than the [1]silatropicenophane **1**, and this is confirmed by the observation of a smaller tilt angle α (22.9° in **2** vs 24.1° in **1**) together with a larger angle δ (161.0° in **2** vs 160.5° in **1**) at the metal center defined by the ring centroids. The same trend has been observed for the structurally characterized Si/Ge couples, the ferrocenophanes **3/4**,^{22,23} and the chromarenophanes **5/6**,^{29,30} (Figure 3, Table 2). It can be clearly concluded that both **1** and **2** represent the most strongly distorted sandwich complexes in comparison to the silylene- and germylene-bridged derivatives shown in Figure 3. For instance, a pronounced decrease in strain is observed on going from the 16-electron [1]silatropicenophane **1** ($\alpha = 24.1^\circ$, $\delta = 160.5^\circ$) to the 17-electron [1]silatrovacenophane **7** ($\alpha = 17.3^\circ$, $\delta = 167.0^\circ$)³¹ and to the [1]silatrochromenophane **8** ($\alpha = 15.6^\circ$, $\delta = 168.4^\circ$),³² which is undoubtedly a consequence of the larger interannular distance in $[(\eta\text{-C}_7\text{H}_7)\text{Ti}(\eta\text{-C}_5\text{H}_5)]$ (tropicene, 3.48 Å)²⁵ compared

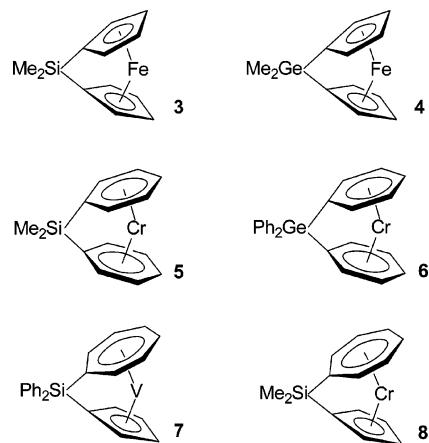


Figure 3. Selected silylene- and germylene-bridged ansa-complexes.

to that in $[(\eta\text{-C}_7\text{H}_7)\text{V}(\eta\text{-C}_5\text{H}_5)]$ (trovacene, 3.38 Å)³³ and in $[(\eta\text{-C}_7\text{H}_7)\text{Cr}(\eta\text{-C}_5\text{H}_5)]$ (trochrocene, 3.26 Å).²⁵

Large angles β and β' are observed for **1** (42.3°, 29.2°) and **2** (41.4°, 28.5°), indicating a strong distortion from planarity at the *ipso*-carbon atoms (Table 2). These values are only exceeded by the corresponding angles found in the vanadium and chromium congeners **7** (48.3° and 32.6°) and **8** (47.7° and 30.6°). This trend, however, must not necessarily impose higher strain on these sandwich molecules in comparison to **1**, since a significant out-of-plane displacement of the substituents of the Cht ring can also partially be attributed to a reorientation of the large seven-membered ring for a better overlap with the smaller vanadium and chromium atoms.^{10,34} Finally, the C1–Si–C5 and C1–Ge–C5 angles in **1** [$\theta = 95.57(13)^\circ$] and **2** [$\theta = 92.76(8)^\circ$] are substantially smaller than expected for ideally sp^3 -hybridized Si and Ge atoms. According to Bent's rule,³⁵ this distortion results in a scissoring effect with a widening of the adjacent angles between the methyl groups and the Si and Ge atoms [C8–Si–C8a = 110.40(15)°, C8–Ge–C8a = 112.03–(11)°].

DSC Studies and Theoretical Investigations on 1 and 2. The structural parameters ascribed to **1** and **2** indicate that these molecules are highly strained, which makes them suitable precursors to metallopolymer via ring-opening polymerization. In a preliminary communication,¹⁵ we reported that **1** is readily transferred into poly(troticenyilsilanes) by heating the monomer at elevated temperatures. On the basis of our differential scanning (DSC) calorimetry studies, the strain energy of **1** was estimated to be about 36 kJ mol⁻¹. Since no melt endotherm had been observed for **1**, this value could have been underestimated due to simultaneous melting and polymerization of the sample. Herein, a reinvestigation of the thermal behavior of **1** together with that of **2** is reported, and Figure 4 shows the differential scanning calorimetry traces of both monomers. While the DSC trace of **1** now shows a perceptible melt endotherm with a maximum at about 155 °C, which merges into an exothermic polymerization signal at 170 °C, the DSC trace of **2** exhibits only one exotherm with its maximum at 130 °C. The observation that **2** polymerizes at lower temperature than **1** is in agreement with the onset polymerization temperatures found for **3** (ca. 120 °C)³⁶ and **4** (ca. 90 °C)²² (Figure 3). This behavior can be attributed to the weaker germanium–carbon bond compared to the silicon–carbon bond,^{30,37} implying that rupture of the interannular link occurs more readily for the Me₂Ge than the Me₂Si bridge. Integration of the exotherms in Figure 4 gives an estimate of the strain energies of ca. 45 kJ mol⁻¹ for both **1** and **2**. It should be noted, however, that these values are presumably underrated, since melting and polymerization of both compounds occur in the same temperature range.

(27) Harrod, J. F.; Malek, A.; Rochon, F. D.; Melanson, R. *Organometallics* **1978**, *6*, 2117.

(28) Marsh, R. E. *Acta Crystallogr.* **1997**, *53b*, 317.

(29) Hultsch, K.; Nelson, J. M.; Lough, A. J.; Manners, I. *Organometallics* **1995**, *14*, 5496.

(30) Eلسchenbroich, C.; Schmidt, E.; Gondrum, R.; Metz, B.; Burghaus, O.; Massa, W.; Wocadlo, S. *Organometallics* **1997**, *16*, 4589.

(31) Eلسchenbroich, C.; Paganelli, F.; Nowotny, M.; Neumüller, B.; Burghaus, O. *Z. Anorg. Allg. Chem.* **2004**, *630*, 1500.

(32) Bartole-Scott, A.; Braunschweig, H.; Kupfer, T.; Lutz, M.; Manners, I.; Nguyen, T.; Radacki, K.; Seeler, F. *Chem.–Eur. J.* **2006**, *12*, 1266.

(33) Engebretson, G.; Rundle, R. E. *J. Am. Chem. Soc.* **1963**, *85*, 481.

(34) Elian, M.; Chen, M. M. L.; Mingos, D. M. P.; Hoffmann, R. *Inorg. Chem.* **1976**, *15*, 1148.

(35) Bent, H. A. *Chem. Rev.* **1961**, *61*, 275.

(36) Foucher, D. A.; Tang, B. Z.; Manners, I. *J. Am. Chem. Soc.* **1992**, *114*, 6246.

(37) (a) Skinner, H. A. *Adv. Organomet. Chem.* **1964**, *2*, 49. (b) Quane, D. *J. Inorg. Nucl. Chem.* **1971**, *33*, 2722.

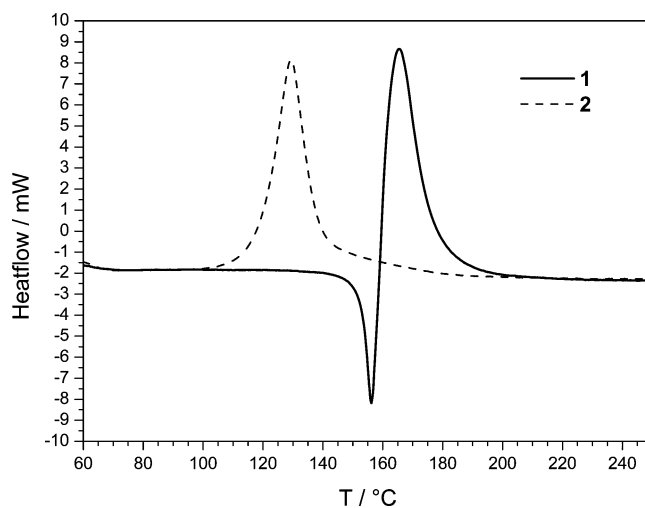


Figure 4. DSC thermograms of **1** (full line) and **2** (dotted line) in the range between 60 and 250 °C; heating rate 10 K min⁻¹.

Despite this limitation, both values are clearly substantially smaller than those found for [Me₂Si(η-C₅H₄)₂Fe] (ca. 80 kJ mol⁻¹)³⁶ and also for chalcogen-bridged [1]ferrocenophanes such as [S(η-C₅H₄)₂Fe] (ca. 130 kJ mol⁻¹) and [Se(η-C₅H₄)₂Fe] (ca. 100 kJ mol⁻¹)³⁸ or for the boron-bridged [iPr₂NB(η-C₅H₄)₂Fe] (ca. 95 kJ mol⁻¹).³⁹ In contrast to **1** and **2**, [(η-C₅H₄)-Ph₂Si-(η-C₇H₆)V] (**7**) and [(η-C₅H₄)-Me₂Si-(η-C₇H₆)Cr] (**8**) decomposed on heating instead of polymerizing.^{31,32}

To further explain the different strain energies of troticenophanes and ferrocenophanes, we performed DFT (density functional theory) calculations for ferrocene and troticene with the Gaussian 03 program suite⁴⁰ using the Becke3LYP density functional⁴¹ and the 6-311G(d,p) basis set combination.⁴² Starting from an unperturbed sandwich structure, where the π-ligands adopt a perfectly coplanar orientation ($\delta = 180^\circ$), the carbocyclic ligands of both complexes were gradually bent along their centroid–metal–centroid axes in 5° intervals with retention of the symmetry (C_s for troticene and C_{2v} for ferrocene). While fixing the positions of the two carbon atoms that lie in the mirror plane bisecting the molecules, all geometries were optimized and the calculated relative energies

(38) Rulkens, R.; Gates, D. P.; Balaishis, D.; Pudelski, J. K.; McIntosh, D. F.; Lough, A. J.; Manners, I. *J. Am. Chem. Soc.* **1997**, *119*, 10976.

(39) (a) Braunschweig, H.; Dirk, R.; Müller, M.; Nguyen, P.; Resendes, R.; Gates, D. P.; Manners, I. *Angew. Chem., Int. Ed. Engl.* **1997**, *36*, 2338. (b) Berenbaum, A.; Braunschweig, H.; Dirk, R.; Englert, U.; Green, J. C.; Jaekle, F.; Lough, A.; Manners, I. *J. Am. Chem. Soc.* **2000**, *122*, 5765.

(40) Frisch, M. J.; Trucks, G. W.; Schlegel, H. B.; Scuseria, G. E.; Robb, M. A.; Cheeseman, J. R.; Montgomery, J. A., Jr.; Vreven, T.; Kudin, K. N.; Burant, J. C.; Millam, J. M.; Iyengar, S. S.; Tomasi, J.; Barone, V.; Mennucci, B.; Cossi, M.; Scalmani, G.; Rega, N.; Petersson, G. A.; Nakatsuji, H.; Hada, M.; Ehara, M.; Toyota, K.; Fukuda, R.; Hasegawa, J.; Ishida, M.; Nakajima, T.; Honda, Y.; Kitao, O.; Nakai, H.; Klene, M.; Li, X.; Knox, J. E.; Hratchian, H. P.; Cross, J. B.; Bakken, V.; Adamo, C.; Jaramillo, J.; Gomperts, R.; Stratmann, R. E.; Yazyev, O.; Austin, A. J.; Cammi, R.; Pomelli, C.; Ochterski, J. W.; Ayala, P. Y.; Morokuma, K.; Voth, G. A.; Salvador, P.; Dannenberg, J. J.; Zakrzewski, V. G.; Dapprich, S.; Daniels, A. D.; Strain, M. C.; Farkas, O.; Malick, D. K.; Rabuck, A. D.; Raghavachari, K.; Foresman, J. B.; Ortiz, J. V.; Cui, Q.; Baboul, A. G.; Clifford, S.; Cioslowski, J.; Stefanov, B. B.; Liu, G.; Liashenko, A.; Piskorz, P.; Komaromi, I.; Martin, R. L.; Fox, D. J.; Keith, T.; Al-Laham, M. A.; Peng, C. Y.; Nanayakkara, A.; Challacombe, M.; Gill, P. M. W.; Johnson, B.; Chen, W.; Wong, M. W.; Gonzalez, C.; Pople, J. A. *Gaussian 03*, Revision C.02; Gaussian, Inc.: Wallingford, CT, 2004.

(41) (a) Becke, A. D. *J. Chem. Phys.* **1993**, *98*, 5648. (b) Miehlich, B.; Savin, A.; Stoll, H.; Preuss, H. *Chem. Phys. Lett.* **1989**, *157*, 200. (c) Lee, C.; Yang, W.; Parr, G. *Phys. Rev. B* **1988**, *37*, 785.

(42) (a) Krishnan, R.; Binkley, J. S.; Seeger, R.; Pople, J. A. *J. Chem. Phys.* **1980**, *72*, 650. (b) McLean, A. D.; Chandler, G. S. *J. Chem. Phys.* **1980**, *72*, 5639. (c) Wachters, A. J. H. *J. Chem. Phys.* **1970**, *52*, 1033.

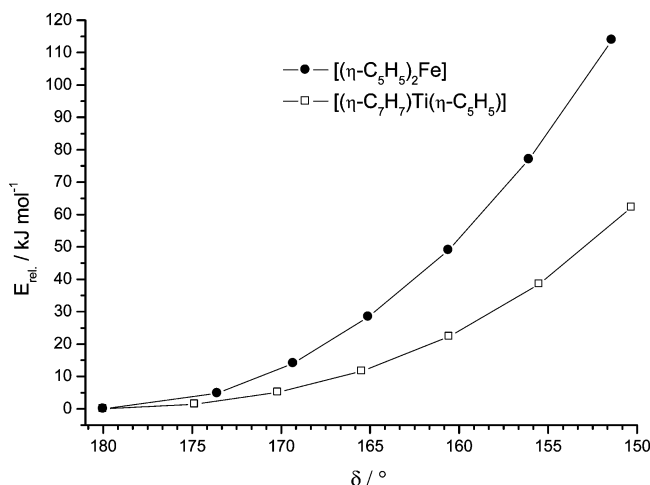
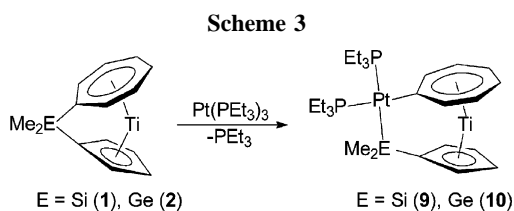


Figure 5. Dependency of the theoretically observed relative energies (kJ mol^{-1}) for ferrocene and trolitene on the angle δ .



were plotted against the angle δ obtained after optimization. As expected, Figure 5 demonstrates that bending of both sandwich molecules results in an exponential increase of energy.⁴³ For ferrocene, however, a significantly steeper rise in energy is observed upon lowering δ , and it can be clearly deduced that distortion of the $[(\eta\text{-C}_5\text{H}_5)_2\text{Fe}]$ moiety requires significantly more energy than that of $[(\eta\text{-C}_5\text{H}_5)\text{Ti}(\eta\text{-C}_7\text{H}_7)]$. As a consequence, the energy released by conversion of a strained into an unstrained molecule is in fact expected to be higher for ferrocenophanes than for troliteneophanes, as has been demonstrated experimentally by the ring-opening polymerization energies determined for the [1]silatroliteneophane **1** (ca. -45 kJ mol^{-1}) and the [1]silaferrrocenophane **3** (ca. -80 kJ mol^{-1}).

Reaction of 1 and 2 with Tris(triethylphosphine)platinum-(0), $[\text{Pt}(\text{PEt}_3)_3]$. Strained metallocenophanes such as $[\text{Me}_2\text{Si}(\eta\text{-C}_5\text{H}_4)_2\text{Fe}]$ had been thoroughly investigated with respect to their ring-opening polymerization behavior, which can be induced either thermally³⁶ or by anionic⁴⁴ or late transition metal catalysis.⁴⁵ For the latter, it has been reported that the initial step of the ROP involves the insertion of the transition metal into the strained Si–C bond,^{45,46} analogous to the proposed mechanism for the transition metal-catalyzed ROP of silacyclobutanes.⁴⁷ In preliminary publications, Braunschweig et al. and our group have independently reported the reaction of **1**

(43) Green, J. C. *Chem. Soc. Rev.* **1998**, 27, 263.

(44) (a) Ni, Y.; Rulkens, R.; Manners, I. *J. Am. Chem. Soc.* **1996**, 118, 4102. (b) Rulkens, R.; Lough, A. J.; Manners, I.; Lovelace, S. R.; Grant, C.; Geiger, W. E. *J. Am. Chem. Soc.* **1996**, 118, 12683. (c) Jäkle, F.; Rulkens, R.; Zech, G.; Massey, J. A.; Manners, I. *J. Am. Chem. Soc.* **2000**, 122, 4231.

(45) (a) Temple, K.; Lough, A. J.; Sheridan, J. B.; Manners, I. *J. Chem. Soc., Dalton Trans.* **1998**, 2799. (b) Temple, K.; Jäkle, F.; Sheridan, J. B.; Manners, I. *J. Am. Chem. Soc.* **2001**, 123, 1355. (c) Chan, W. Y.; Berenbaum, A.; Clendenning, S. B.; Lough, A. J.; Manners, I. *Organometallics* **2003**, 22, 3796.

(46) (a) Sheridan, J. B.; Lough, A. J.; Manners, I. *Organometallics* **1996**, 15, 2195. (b) Reddy, N. P.; Choi, N.; Shimada, S.; Tanaka, M. *Chem. Lett.* **1996**, 649. (c) Sheridan, J. B.; Temple, K.; Lough, A. J.; Manners, I. *J. Chem. Soc., Dalton Trans.* **1997**, 711. (d) Temple, K.; Jäkle, F.; Lough, A. J.; Sheridan, J. B.; Manners, I. *Polym. Preprints* **2000**, 41, 429.

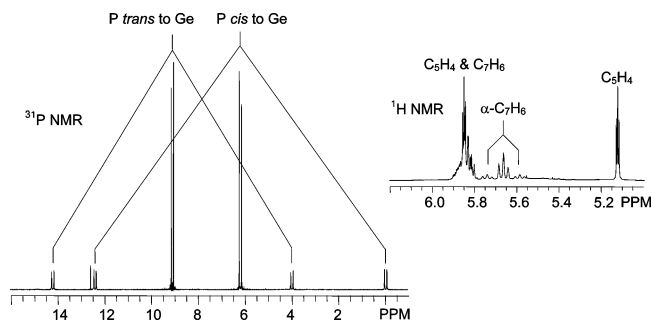


Figure 6. Portions of the ^{31}P and the ^1H NMR spectra of **10**.

and of the vanadium and chromium congeners $[(\eta\text{-C}_5\text{H}_4)\text{-Me}_2\text{-Si}(\eta\text{-C}_7\text{H}_6)\text{V}]$ and $[(\eta\text{-C}_5\text{H}_4)\text{-Me}_2\text{Si}(\eta\text{-C}_7\text{H}_6)\text{Cr}]$ with equivalent amounts of tris(triethylphosphine)platinum(0)⁴⁸ and were able to demonstrate the regioselective insertion of a $[\text{Pt}(\text{PEt}_3)_2]$ moiety into the silicon–carbon bond to the seven-membered ring.^{14,32} However, no detailed structural comparison has been accomplished yet. In this contribution, we would like to give a full experimental report on the reactivity of **1** and **2** toward $[\text{Pt}(\text{PEt}_3)_3]$ and discuss their structural and spectroscopic properties in comparison to related systems.

Treatment of toluene solutions of **1** and **2** with equivalent amounts of $[\text{Pt}(\text{PEt}_3)_3]$ results in an instantaneous color change from blue to green, and the resulting [2]trotiteneophanes **9** and **10** could be obtained in yields up to 76% after workup with hexane. Both compounds were characterized by means of multinuclear NMR spectroscopy, elemental analysis, and mass spectrometry. The ^{31}P NMR spectrum of **9** exhibits two signals at 11.2 (*trans* to silicon) and 8.5 ppm (*cis* to silicon), indicating a square planar environment at the platinum center. Because of ^{31}P – ^{31}P coupling, both resonances are split into two doublets with $^2J_{\text{PP}} = 17.0 \text{ Hz}$. Furthermore, these resonances show large ^{31}P – ^{195}Pt coupling constants of 994 and 2108 Hz, respectively. The different coupling constants can be explained by the strong *trans* influence of the silyl substituent, as was also observed for the related [2]platinasilaferrrocenophane $[(\eta\text{-C}_5\text{H}_4)\text{-Pt}(\text{PEt}_3)_2\text{-Me}_2\text{Si}(\eta\text{-C}_5\text{H}_4)\text{Fe}]$ ^{46a,b} and [2]platinasilatrotiteneophane $[(\eta\text{-C}_5\text{H}_4)\text{-Pt}(\text{PEt}_3)_2\text{-Me}_2\text{Si}(\eta\text{-C}_7\text{H}_6)\text{Cr}]$ ($\delta = 9.1, 8.9$; $^2J_{\text{PP}} = 17 \text{ Hz}$; $^2J_{\text{PPt}} = 1028, 2007 \text{ Hz}$).³² Similarly, the ^{31}P NMR spectrum of **10** exhibits two doublets at 9.1 and 6.2 ppm with $^2J_{\text{PP}} = 16.6 \text{ Hz}$ and additional ^{31}P – ^{195}Pt couplings of 1647 and 2013 Hz (Figure 6).

The ^1H NMR spectra of both **9** and **10** show multiplets with Pt satellites for the $\alpha\text{-C}_7\text{H}_6$ protons next to the bridging moiety, which unequivocally confirms that the regioselective insertion into the E–C bond (E = Si, Ge) to the seven-membered ring has occurred. This resonance can be observed at 5.62 ppm for **9** and is found to be slightly downfield shifted to 5.66 ppm in the ^1H NMR spectrum of **10** (Figure 6). The ^1H – ^{195}Pt coupling constants are $^3J_{\text{HPt}} = 67 \text{ Hz}$ for **9** and $^3J_{\text{HPt}} = 62 \text{ Hz}$ for **10**. In the ^{13}C NMR spectra of **9** and **10**, only the carbon resonances of the *ipso*-, α -, and β - C_7H_6 carbon atoms show ^{13}C – ^{31}P couplings. Since the insertion into the heteroatom–carbon bond results in a strain release, the resonance for the *ipso*- C_7H_6 carbon atom in **9** is observed at considerably lower field compared to **1** (89.0 in **9** vs 61.6 ppm in **1**). Unfortunately, this resonance could not be detected for **10**. Finally, the ^{195}Pt NMR spectrum of **9** exhibits an AB spectrum because of ^{195}Pt – ^{31}P coupling of the platinum center with the two chemically different phosphorus

(47) (a) Wu, H. J.; Interrante, L. V. *Macromolecules* **1992**, 25, 1840. (b) Yamashita, H.; Tanaka, M.; Honda, K. *J. Am. Chem. Soc.* **1995**, 117, 8873.

(48) Yoshida, T.; Matsuda, T.; Otsuka, S. *Inorg. Synth.* **1990**, 28, 119.

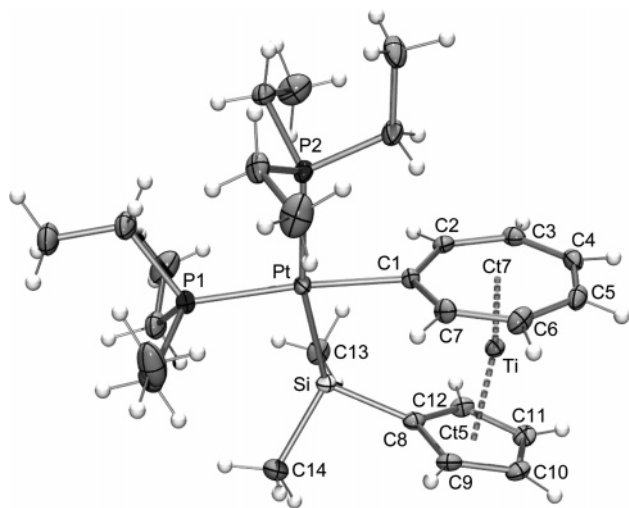
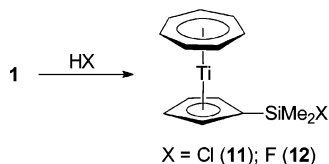


Figure 7. ORTEP-style plot of the molecular structure of **9**. Selected bond lengths [Å] and angles [deg]: Pt–P1 2.2962(9), Pt–P2 2.3874(6), Pt–Si 2.3881(8), Pt–C1 2.096(3), Ti–C1 2.196(3), Ti–C2 2.199(3), Ti–C3 2.212(3), Ti–C4 2.215(3), Ti–C5 2.216(3), Ti–C6 2.196(3), Ti–C7 2.184(3), Ti–C8 2.280(3), Ti–C9 2.293(3), Ti–C10 2.333(3), Ti–C11 2.333(3), Ti–C12 2.301(3), Si–C8 1.890(3), P1–Pt–P2 99.42(3), P1–Pt–Si 92.42(3), P2–Pt–C1 84.66(9), Si–Pt–C1 83.70(9).

Scheme 4



nuclei, and this resonance is found at -4630.0 ppm. This chemical shift is in agreement with the ^{195}Pt NMR spectrum of the related ferrocene derivative $[(\eta\text{-C}_5\text{H}_4)\text{-Pt}(\text{PET}_3)_2\text{-Me}_2\text{Si}(\eta\text{-C}_5\text{H}_4)\text{Fe}]$, which exhibits a doublet of doublets at -4661.0 ppm.^{45a}

Figure 7 shows an ORTEP-style plot of the previously determined¹⁴ molecular structure of **9**, and Table 3 summarizes the structural parameters in comparison to the [2]platinasilatrovacenophane and [2]platinasilatrochrocenophane congeners.^{14,32} All three compounds are isotopic and crystallize in the orthorhombic space group $P2_12_12_1$. As expected from the crystal structures of the parent complexes $[(\eta\text{-C}_7\text{H}_7)\text{M}(\eta\text{-C}_5\text{H}_5)]$ ($\text{M} = \text{Ti}, \text{V}, \text{Cr}$),²⁵ the metal–carbon bond distances decrease in the order $\text{Ti} > \text{V} > \text{Cr}$. Accordingly, **9** shows the strongest deviation from an unstrained sandwich structure with $\alpha = 13.5^\circ$ and $\delta = 169.1^\circ$. Smaller angles α together with larger angles δ are consequently observed for the vanadium ($\alpha = 10.6^\circ$, $\delta = 171.9^\circ$) and chromium analogues ($\alpha = 7.5^\circ$, $\delta = 174.9^\circ$). In all complexes, the platinum centers are in a slightly distorted square planar environment with two different PEt_3 ligands. Because of the strong *trans* influence of the silyl substituents, the Pt–P2 distances are significantly longer than Pt–P1. These distances and also the Pt–C1 and Pt–Si bond lengths are in reasonable agreement with the values obtained from structural characterization of related [2]platinasilaferrrocenophanes.⁴⁶

Protonolysis Reactions with 1 and 2. It has been reported for strained [1]ferrocenophanes $[\text{R}_2\text{E}(\eta\text{-C}_5\text{H}_4)_2\text{Fe}]$ that the reaction with protic acids such as HOTf, HCl, and HBF_4 results in the cleavage of one heteroatom–carbon bond and formation of relaxed sandwich compounds of the type $[(\eta\text{-C}_5\text{H}_5)\text{Fe}(\eta\text{-C}_5\text{H}_4\text{SiR}_2\text{X})]$ ($\text{X} = \text{F}, \text{Cl}, \text{OTf}$), allowing convenient access to

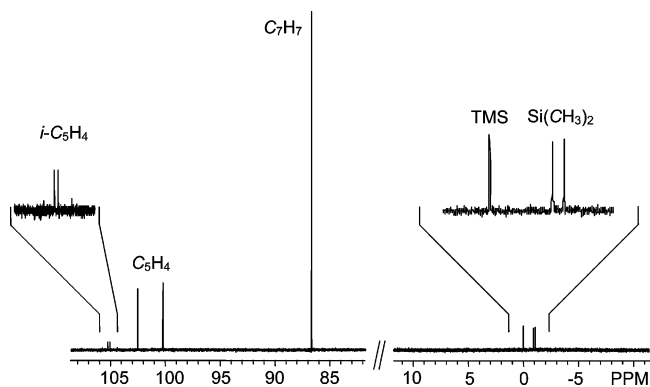


Figure 8. Portion of the ^{13}C NMR spectrum of **12** in benzene- d_6 .

Table 3. Structural Comparison of Titanium, Vanadium, and Chromium Complexes of the Type $[(\text{PET}_3)_2\text{PtSiMe}_2(\eta\text{-C}_7\text{H}_6)\text{M}(\eta\text{-C}_5\text{H}_4)]^a$

	M = Ti (9)	M = V	M = Cr
M–C ₇ ^b	1.468	1.446	1.411
M–C ₇ ^c			
average	2.203	2.184	2.149
range	2.184(3)–2.216(3)	2.168(3)–2.192(3)	2.141(4)–2.173(4)
C ₇ –C ₇ ^c			
average	1.420	1.420	1.407
range	1.404(5)–1.432(5)	1.411(4)–1.431(4)	1.391(6)–1.421(6)
M–C ₅ ^d	1.967	1.888	1.808
M–C ₅ ^e			
average	2.308	2.242	2.174
range	2.280(3)–2.333(3)	2.209(3)–2.274(3)	2.150(4)–2.201(4)
C ₅ –C ₅ ^e			
average	1.425	1.421	1.421
range	1.417(5)–1.430(5)	1.408(4)–1.433(4)	1.409(6)–1.434(6)
Pt–P1	2.2962(9)	2.3020(7)	2.3057(12)
Pt–P2	2.3874(6)	2.3849(6)	2.3745(10)
Pt–Si	2.3881(8)	2.3900(6)	2.4229(13)
Pt–C1	2.096(3)	2.092(2)	2.087(4)
Si–C8	1.890(3)	1.894(3)	1.895(5)
P1–Pt–P2	99.42(3)	99.38(2)	99.34(4)
P1–Pt–Si	92.42(3)	92.37(2)	92.51(4)
P2–Pt–Si	167.00(3)	166.95(3)	166.42(4)
P1–Pt–C1	175.54(9)	175.31(7)	174.58(11)
P2–Pt–C1	84.66(9)	84.89(7)	85.63(11)
Si–Pt–C1	83.70(9)	83.59(7)	82.82(11)
α	13.5	10.6	7.5
δ	169.1	171.9	174.9

^a Bond lengths in Å. ^bC₇ = centroid of the seven-membered ring. ^cC₇ = carbon atom of the seven-membered ring. ^dC₅ = centroid of the five-membered ring. ^eC₅ = carbon atom of the five-membered ring.

ferrocenylchlorosilanes and -germanes.⁴⁹ Furthermore, low-temperature NMR studies indicated that addition of protic acids with weakly coordinating anions such as $[\text{H}(\text{Et}_2\text{O})_2][(\text{3,5}(\text{CF}_3)_2\text{C}_6\text{H}_3)_4\text{B}]^{50}$ to [1]ferrocenophanes generates cationic species with silylium character.^{49b,51} In order to investigate the reactivity of *ansa*-Cht–Cp complexes toward protic acids, the reaction of **1** with 1 equiv of HCl and HBF_4 was carried out (Scheme 4).

Treatment of **1** with a stoichiometric amount of HCl dissolved in diethyl ether results in an immediate color change from blue to green, and a green crystalline solid was isolated after recrystallization from a thf/hexane mixture. The ^1H NMR spectrum of the product in benzene- d_6 shows two singlet signals

(49) (a) MacLachlan, M. J.; Ginzburg, M.; Knöll, O.; Lough, A. J.; Manners, I. *New J. Chem.* **1998**, 1409. (b) Bourke, S. C.; MacLachlan, M. J.; Lough, A. J.; Manners, I. *Chem.–Eur. J.* **2005**, *11*, 1989.

(50) Brookhart, M.; Grant, B.; Volpe, A. F., Jr. *Organometallics* **1992**, *11*, 3920.

(51) MacLachlan, M. J.; Bourke, S. C.; Lough, A. J.; Manners, I. *J. Am. Chem. Soc.* **2000**, *122*, 2126.

at 5.41 and 5.06 ppm with an integrated ratio of 7:4, indicating that a regioselective protonolysis of the Si–C₇H₆ bond to the seven-membered ring and formation of the trocticene derivative [(η -C₇H₇)Ti(η -C₅H₄SiMe₂Cl)] (**11**) must have occurred. The structure of **11** could be unambiguously confirmed from the ¹³C NMR spectrum, which shows four signals attributable to the carbocyclic ligands. Whereas the carbon atoms of the five-membered ring give rise to separated resonance signals at 100.5, 102.5, and 105.7 ppm (*ipso*), only one high-field resonance at 86.9 ppm is observed for the seven-membered ring carbon atoms, which falls in the same range as the corresponding resonance for trocticene (84.3 ppm). In a similar way, the reaction of **1** with an ethereal HBF₄ solution has been carried out. On addition of the acid to a thf solution of **1**, a color change from blue to green-blue was observed, and the fluorosilane [(η -C₇H₇)Ti(η -C₅H₄SiMe₂F)] (**12**) was isolated as a blue-green solid after crystallization from thf/hexane. The new compound was characterized by means of ¹H, ¹³C, ²⁹Si, and ¹⁹F NMR spectroscopy. The ¹H NMR spectrum shows two resonances for the C₇H₇ and C₅H₄ hydrogen atoms at 5.43 and 5.08 ppm, respectively, together with a doublet at 0.24 ppm for the methyl groups attached to silicon. The ¹³C NMR spectrum exhibits one signal for the Cht ligand at 86.7 ppm and three resonances for the Cp carbon atoms at 100.3, 102.6, and 105.2 ppm (Figure 7). The latter is split into a doublet by ¹³C–¹⁹F coupling (²J_{CF} = 18.7 Hz). A separation into a doublet can also be observed for the ¹³C NMR resonance of the methyl groups at the silicon atom (–0.9 ppm, ²J_{CF} = 16.8 Hz).

The ¹⁹F and ²⁹Si NMR spectra of **12** exhibit one resonance each at –151.1 and 15.8 ppm, respectively, and from both signals, a ¹⁹F–²⁹Si coupling constant of ¹J_{SiF} = 276 Hz can be deduced. For comparison, the ferrocene analogue [(η -C₅H₅)Fe(η -C₅H₄SiMe₂F)] shows the respective signals at –150.2 and 23.6 ppm with ¹J_{SiF} = 272 Hz.^{49b} The formation of **12** presumably proceeds via a highly reactive silyl cation intermediate with the formulation [(η -C₇H₇)Ti(η -C₅H₄SiMe₂)]⁺, which is able to extract F[–] from the tetrafluoroborate counteranion. This mechanism has already been postulated by Manners et al. for the reaction of [1]silaferrocenophanes with HBF₄.^{49b}

Conclusions

With this contribution, we have shown that the reaction of lithiated trocticene [(η -C₇H₆Li)Ti(η -C₅H₄Li)] with Me₂SiCl₂ and Me₂GeCl₂ leads to the formation of *ansa*-Cht–Cp complexes, namely, the [1]silaferrocenophane **1** and [1]germatrocticenophane **2**. The resulting compounds are highly strained molecules, and DSC studies reveal that **1** and **2** can be readily converted into the corresponding poly(trocticenylsilanes) and -germanes via the thermally induced ring-opening polymerization. It is particularly noteworthy that all metal insertion and protonolysis reactions of **1** and **2** presented here proceed exclusively via regioselective cleavage of the E–C bonds (E = Si, Ge) to the seven-membered ring, which could be a result of the strong distortion at the E–C₇H₆ site. Hence, the selective formation of the [2]-platinasila- and [2]platinagermatrocticenophanes **9** and **10** suggests that **1** and **2** represent suitable precursors for the metal-catalyzed generation of regioregular polytrocticenes.¹⁴ In a similar fashion, the selective E–C bond cleavage by HCl and HBF₄ and exclusive formation of trocticenes of the type [(η -C₇H₇)Ti(η -C₅H₄SiMe₂X)] (**11**, X = Cl; **12**, X = F) allows access to Cp-substituted trocticenes, which might be useful for further developments in this field.

Experimental Details

General Methods. All operations were performed in an atmosphere of dry argon by using Schlenk and vacuum techniques. Solvents were dried by standard methods and distilled prior to use. Trocticene⁵² and [Pt(PEt₃)₃]⁴⁸ were prepared according to published procedures. Elemental analyses (C, H, N) were performed on a Elementar Vario EL III and a Vario Micro Cube elemental analyzer. ¹H and ¹³C NMR spectra were measured on Jeol JNM GX 400, Bruker AV 300, and Bruker DRX 400 spectrometers using the solvent as internal standard. The assignment of all resonances was supported by two-dimensional NMR spectroscopy (COSY, HMBC, HSQC, and COLOC experiments). The ²⁹Si NMR, ¹⁹F NMR, ³¹P NMR, and ¹⁹⁵Pt NMR spectra were referenced to the signals of SiMe₄, CFCl₃, H₃PO₄ (85%), and H₂PtCl₆ in D₂O, respectively. Mass spectrometry (EI and HR-MS) has been performed on a Finnigan MAT 90 device. Accurate mass measurements refer to the monoisotopic peak of the isotopic pattern. The differential scanning calorimetry (DSC) measurements of compound **1** and **2** were performed on a Rheometric Scientific device (DSC SP) under a continuous flow of argon with a heating rate of 10 K/min. The internal calibration was carried out by measuring the melt enthalpies of Sn, RbNO₃, KClO₄, Zn, and Ag₂SO₄, respectively.

Synthesis of [Me₂Si(η -C₇H₆)Ti(η -C₅H₄)] (1**).** A solution of *n*-butyllithium (25 mL of a 2.5 M solution in hexane, 62.5 mmol) and tmeda (73.5 mmol, 11.1 mL) in 80 mL of hexane was slowly treated with solid trocticene (24.5 mmol, 5.0 g) and stirred overnight. The resulting brownish slurry, containing [(η -C₇H₆Li)Ti(η -C₅H₄-Li)]·2tmeda, was cooled to –78 °C, and a solution of dichlorodimethylsilane (49.3 mmol, 6.0 mL) in 150 mL of hexane was added dropwise over a period of 6 h. The reaction mixture was allowed to reach ambient temperature overnight. After filtration through Celite, the solvent was removed in vacuo. The oily residue was suspended in a few milliliters of hexane, and the solvent decanted off via a cannula. Drying the residue in high vacuum afforded **1** as a blue-green solid, which can be purified by crystallization from a thf/hexane mixture at –78 °C. Single crystals of compound **1** were obtained by slow cooling of a saturated solution in THF. Yield: 2.5 g (39%). Anal. Calcd for C₁₄H₁₆SiTi: C, 64.61; H, 6.20. Found: C, 64.57; H, 6.22. ¹H NMR (400 MHz, C₆D₆): δ 5.89 (m, 4H, β - and γ -C₇H₆), 4.87 (m, 4H, C₅H₄), 4.75 (dm, 2H, α -C₇H₆), 0.41 (s, 6H, (CH₃)₂Si). ¹³C{¹H} NMR (100 MHz, C₆D₆): δ 101.2 (β -C₇H₆), 101.0 (C₅H₄), 100.6 (C₅H₄), 89.7 (γ -C₇H₆), 87.6 (α -C₇H₆), 83.6 (*i*-C₅H₄), 61.6 (*i*-C₇H₆), –5.9 (Si(CH₃)₂). ²⁹Si NMR (53.67 MHz, C₆D₆): δ –4.23 (Si(CH₃)₂). MS (CI): 260, (M⁺) 245, (M⁺ – CH₃) 230, (M⁺ – (CH₃)₂) 202, (M⁺ – Si(CH₃)₂). HR-MS (EI; *m/z*): calcd for C₁₄H₁₆SiTi (M⁺), 258.0548; found, 258.0548. UV/vis (CH₂Cl₂): λ_{\max} (ϵ) = 663 (105).

Synthesis of [Me₂Ge(η -C₇H₆)Ti(η -C₅H₄)] (2**).** A solution of *n*-butyllithium (23.0 mL of a 1.6 M solution in hexane, 36.7 mmol) and tmeda (5.12 g, 6.65 mL, 44.1 mmol) in 60 mL of hexane was treated with solid trocticene (3.0 g, 14.7 mmol) and stirred for 24 h. The resulting dark brown suspension, containing [(C₇H₆Li·tmeda)-Ti(C₅H₄Li·tmeda)], was cooled to –78 °C, and a precooled (–78 °C) hexane solution of dimethyl(dichloro)germane (3.83 g, 2.54 mL, 22.0 mmol in 120 mL of hexane) was added dropwise within a period of 6 h. The reaction mixture was allowed to reach ambient temperature overnight, and the solution was separated from the residue by filtration over Celite. The solvent of the filtrate was removed in vacuo and the resulting blue-green sticky solid purified by crystallization at –25 °C from a hexane/thf mixture (2:1). Crystals for X-ray diffraction could be obtained by slow cooling of a saturated solution in toluene to –35 °C. Yield: 0.806 g (18%). Anal. Calcd for C₁₄H₁₆GeTi: C, 55.18; H, 5.29; Found: C, 55.01;

(52) (a) van Oven, H. O.; Liefde Meijer, H. J. *J. Organomet. Chem.* **1970**, *23*, 159. (b) Demerseman, B.; Dixneuf, P. H.; Douglade, J.; Mercier, R. *Inorg. Chem.* **1982**, *21*, 3942.

H, 5.23. ^1H NMR (400 MHz, C_6D_6): δ 5.96 (m, 2H, β - C_7H_6), 5.88 (m, 2H, γ - C_7H_6), 4.95 (m, 2H, C_5H_4), 4.87 (m, 2H, C_5H_4), 4.76 (m, 2H, β - C_7H_6), 0.50 (s, 6H, $(\text{CH}_3)_2\text{Ge}$). $^{13}\text{C}\{\text{H}\}$ NMR (100 MHz, C_6D_6): δ 100.7 (C_5H_4), 100.5 (C_5H_4), 100.3 (β - C_7H_6), 89.5 (γ - C_7H_6), 88.6 (α - C_7H_6), 81.6 (i - C_5H_4), 58.8 (i - C_7H_6), -6.0 ($(\text{CH}_3)_2\text{Ge}$). MS (EI): 306, (M^+) 291, ($\text{M}^+ - \text{CH}_3$) 276, ($\text{M}^+ - (\text{CH}_3)_2$) 202, ($\text{M}^+ - \text{Ge}(\text{CH}_3)_2$). HR-MS (EI; m/z): calcd for $\text{C}_{14}\text{H}_{16}\text{GeTi}$ (M^+), 300.0021; found, 300.0013.

Synthesis of [(PEt₃)₂PtSiMe₂(η -C₇H₆)Ti(η -C₅H₄)] (9). A solution of **1** (0.074 g, 0.28 mmol) in 20 mL of toluene was added dropwise to a solution of Pt(PEt₃)₃ (0.155 g, 0.28 mmol) in 20 mL of toluene at room temperature. The resulting green solution was evaporated to dryness, and the residue was extracted with 40 mL of hexane. Evaporation of the extract to 2 mL and subsequent cooling to -25 °C afforded **9** as a green crystalline solid. Yield: 0.056 g (26%). Anal. Calcd for $\text{C}_{26}\text{H}_{46}\text{P}_2\text{PtSiTi}$: C, 45.15; H, 6.70. Found: C, 45.57; H, 6.85. ^1H NMR (400 MHz, C_6D_6): δ 5.87 (m, 4H, β - C_7H_6 and γ - C_7H_6), 5.78 (m, 2H, α - C_5H_4), 5.62 (m, $^3J_{\text{PH}} = 67$ Hz, 2H, α - C_7H_6), 5.09 (m, 2H, β - C_5H_4), 1.62 (m, 6H, PCH_2CH_3), 1.24 (m, 6H, PCH_2CH_3), 0.93 (m, 9H, PCH_2CH_3), 0.81 (m, 9H, PCH_2CH_3), 0.77 (m, 6H, $^2J_{\text{PH}} = 24$ Hz, $^3J_{\text{PH}} = 2.3$ Hz, SiCH_3). $^{13}\text{C}\{\text{H}\}$ NMR (100 MHz, C_6D_6): δ 120.3 (i - C_5H_4), 102.4 (α - C_5H_4), 97.0 (β - C_5H_4), 91.5 (m, $^2J_{\text{PC}} = 79$ Hz, $^3J_{\text{PP}} = 9.2$ Hz, α - C_7H_6), 90.7 (m, $^3J_{\text{PC}} = 33$ Hz, β - C_7H_6), 89.0 (dd, $^2J_{\text{CP}} = 104$ and 15 Hz, i - C_7H_6), 86.4 (γ - C_7H_6), 18.3 (m, $^2J_{\text{PC}} = 28$ Hz, $^1J_{\text{CP}} = 27$ Hz, $^3J_{\text{CP}} = 5$ Hz, PCH_2CH_3 *trans* to C_7H_6 group), 15.3 (m, $^1J_{\text{CP}} = 17.7$, $^2J_{\text{PC}} = 12.2$ Hz, PCH_2CH_3 *trans* to silyl group), 8.8 (m, $^3J_{\text{PC}} = 22.7$ Hz, PCH_2CH_3 *trans* to C_7H_6), 8.0 (m, $^3J_{\text{PC}} = 10.9$ Hz, PCH_2CH_3 *trans* to silyl group), 7.5 (m, $^2J_{\text{PC}} = 76.8$ Hz, $^3J_{\text{CP}} = 11.7$ and 1.5 Hz, SiCH_3). ^{31}P NMR (C_6D_6): δ 11.23 (m, $^1J_{\text{PP}} = 994$ Hz, $^2J_{\text{SiP}} = 193$ Hz, $^2J_{\text{PP}} = 17$ Hz, PEt_3 *trans* to silyl group), 8.54 (m, $^1J_{\text{PP}} = 2108$ Hz, $^2J_{\text{PP}} = 17$ Hz, PEt_3 *trans* to C_7H_6). ^{195}Pt NMR (C_6D_6): δ -4630 (dd, $^1J_{\text{PP}} = 2109$ Hz, $^1J_{\text{PP}} = 992$ Hz).

Synthesis of [(PEt₃)₂PtGeMe₂(η -C₇H₆)Ti(η -C₅H₄)] (10). A solution of **2** (0.128 g, 0.42 mmol) in 20 mL of toluene was treated dropwise with a solution of Pt(PEt₃)₃ (0.231 g, 0.42 mmol) in 20 mL of toluene at room temperature. The resulting green solution was stirred overnight and evaporated to dryness. The residue was suspended in 40 mL of hexane, isolated by filtration, and washed three times with 5 mL of hexane. Yield: 0.235 g (76%). Anal. Calcd for $\text{C}_{26}\text{H}_{46}\text{P}_2\text{PtGeTi}$: C, 42.42; H, 6.30. Found: C, 42.32; H, 6.33. ^1H NMR (400 MHz, C_6D_6): δ 5.85 (m, 2H, α - C_5H_4), 5.83 (m, 4H, β - C_7H_6 and γ - C_7H_6), 5.66 (m, $^3J_{\text{PH}} = 62$ Hz, 2H, α - C_7H_6), 5.13 (m, 2H, β - C_5H_4), 1.61 (m, 6H, PCH_2CH_3), 1.23 (m, 6H, PCH_2CH_3), 0.92 (m, 9H, PCH_2CH_3), 0.83 (d, 6H, $^3J_{\text{PH}} = 1.8$ Hz, GeCH_3), 0.79 (m, 9H, PCH_2CH_3). $^{13}\text{C}\{\text{H}\}$ NMR (100 MHz, C_6D_6): δ 124.3 (i - C_5H_4), 102.9 (α - C_5H_4), 96.9 (β - C_5H_4), 90.9 (m, $^2J_{\text{PC}} = 33.8$ Hz, $^3J_{\text{PP}} = 2.0$ Hz, α - C_7H_6), 90.6 (m, β - C_7H_6), 86.2 (γ - C_7H_6), 18.2 (m, $^1J_{\text{CP}} = 26.7$ Hz, $^3J_{\text{CP}} = 3.6$ Hz, PCH_2CH_3 *trans* to C_7H_6), 15.6 (m, $^1J_{\text{CP}} = 21.8$, $^3J_{\text{CP}} = 1.6$ Hz, PCH_2CH_3 *trans* to germyl group), 8.8 (m, $^3J_{\text{PC}} = 21.6$ Hz, PCH_2CH_3 *trans* to C_7H_6), 8.0 (m, $^3J_{\text{PC}} = 15.1$ Hz, PCH_2CH_3 *trans* to germyl group), 7.0 (dm, $^3J_{\text{CP}} = 14.5$ Hz, GeCH_3). The i - C_5H_4 resonance could not be observed. $^{31}\text{P}\{\text{H}\}$ NMR (162 MHz, C_6D_6): δ 6.18 (m, $^1J_{\text{PP}} = 1647$ Hz, $^2J_{\text{PP}} = 16.6$ Hz, PEt_3 *trans* to germyl group), 9.07 (m, $^1J_{\text{PP}} = 2013$ Hz, $^2J_{\text{PP}} = 16.6$ Hz, PEt_3 *cis* to germyl group). MS (EI): 736, (M^+) 618, ($\text{M}^+ - \text{PEt}_3$) 603, (618 - CH_3) 589, (618 - C_2H_5) 570, (618 - Ti) 555, (603 - Ti).

Synthesis of [(η -C₇H₇)Ti(η -C₅H₄SiMe₂Cl)] (11). To a solution of 0.133 g (0.51 mmol) of **1** in THF was added dropwise a solution of HCl in diethyl ether (255 μL of a 2 M solution, 0.51 mmol) at room temperature over a period of 15 min. During addition, a color change from blue to green was observed, and the resulting solution was stirred for an additional 2 h at room temperature. The solvent was removed in vacuo and the resulting oily residue extracted with benzene. Subsequent crystallization from THF led to the isolation of **11** in spectroscopically pure form (NMR) as a light blue solid. Yield: 0.110 g (73%). ^1H NMR (400 MHz, C_6D_6): δ 5.41 (s, 7H, C_7H_7), 5.06 (s, 4H, C_5H_4), 0.41 (s, 6H, $\text{Si}(\text{CH}_3)_2\text{Cl}$). $^{13}\text{C}\{\text{H}\}$ NMR (100 MHz, C_6D_6): δ 105.7 (i - C_5H_4), 102.5 (C_5H_4), 100.5 (C_5H_4), 86.9 (C_7H_7), 2.8 ($\text{Si}(\text{CH}_3)_2\text{Cl}$). $^{29}\text{Si}\{\text{H}\}$ NMR (39.80 MHz, C_6D_6): δ 5.1 (SiMe_2Cl). MS (EI): 296, (M^+) 203, ($\text{M}^+ - \text{SiMe}_2\text{Cl}$). HR-MS (EI; m/z): calcd for $\text{C}_{14}\text{H}_{17}\text{ClSiTi}$ (M^+), 294.0314; found, 294.0307.

Synthesis of [(η -C₇H₇)Ti(η -C₅H₄SiMe₂F)] (12). A solution of **1** (0.112 g, 0.430 mmol) in 20 mL of THF was treated dropwise with a solution of tetrafluoroboric acid (0.07 g, 0.430 mmol, 54% in Et_2O) at room temperature. After stirring the resulting green solution for an additional 3 h at room temperature, the solvent was removed in vacuo. The product was isolated in spectroscopically pure form (NMR) after crystallization from a THF/hexane mixture at -25 °C as a blue solid. Yield: 0.093 g (77%). ^1H NMR (400 MHz, C_6D_6): δ 5.43 (s, 7H, C_7H_7), 5.08 (s, 4H, C_5H_4), 0.25 (d, $^3J_{\text{HF}} = 7.0$ Hz, 6H, $\text{Si}(\text{CH}_3)_2\text{F}$). $^{13}\text{C}\{\text{H}\}$ NMR (100 MHz, C_6D_6): δ 105.2 (d, $^2J_{\text{CF}} = 18.6$ Hz, i - C_5H_4), 102.6 (C_5H_4), 100.3 (C_5H_4), 86.7 (C_7H_7), -0.9 (d, $^2J_{\text{CF}} = 16.9$ Hz, $\text{Si}(\text{CH}_3)_2\text{F}$). $^{29}\text{Si}\{\text{H}\}$ NMR (39.8 MHz, C_6D_6): δ 15.8 (d, $^1J_{\text{SiF}} = 276.3$ Hz, SiMe_2F). $^{19}\text{F}\{\text{H}\}$ NMR (376.5 MHz, C_6D_6): δ -151.1 (m, $^1J_{\text{SiF}} = 276.7$ Hz, SiMe_2F). MS (EI): 280, (M^+) 203, ($\text{M}^+ - \text{SiMe}_2\text{F}$).

Single-Crystal X-ray Structure Determination of 2. Crystal data at -140 °C: $\text{C}_{14}\text{H}_{16}\text{TiGe}$, $M = 304.75$, orthorhombic, $Pnma$, $a = 7.4995(6)$ Å, $b = 11.8983(10)$ Å, $c = 13.9878(18)$ Å, $V = 1248.2$ Å³, $Z = 4$. Data collection and refinement: An irregular fragment of ca. $0.3 \times 0.1 \times 0.1$ mm was used to register 23 920 intensities on a Bruker SMART 1000 CCD diffractometer (Mo $K\alpha$ radiation, $\lambda = 0.71073$ Å, $2\theta_{\text{max}} 61^\circ$). An absorption correction ($\mu = 3.0$ mm⁻¹) was performed using multiscans (program SADABS). Averaging equivalents gave 1993 unique reflections ($R_{\text{int}} 0.032$), which were used for all calculations. The structure was refined on F^2 using the program SHELXL-97 (G. M. Sheldrick, University of Göttingen, Germany). Hydrogen atoms were included using a riding model. The final wR_2 was 0.059 for all reflections and 80 parameters, with a conventional R_1 of 0.022; $S = 1.16$, max. $\Delta\rho +0.54/-0.31$ e Å⁻³. Complete data (excluding structure factors) have been deposited at the Cambridge Crystallographic Data Centre under the number CCDC-622653 and can be obtained free of charge from www.ccdc.cam.ac.uk/data_request/cif.

Supporting Information Available: Crystal data in CIF format. This material is available free of charge via the Internet at <http://pubs.acs.org>.

OM060928L